Comparison of Dielectric and Viscoelastic Relaxation Behavior of Polyisoprene Solutions: Coherence in Subchain Motion

Hiroshi Watanabe,*,† Min-Long Yao,‡ and Kunihiro Osaki†

Institute for Chemical Research, Kyoto University, Uji, Kyoto 611, Japan, and Rheometric Scientific F.E. Ltd., 2-19-6 Yanagibashi, Taito-ku, Tokyo 111, Japan

Received July 18, 1995; Revised Manuscript Received October 11, 1995[⊗]

ABSTRACT: Viscoelastic relaxation of polymer chains at long time scales is induced by their global motion. This motion also induces dielectric relaxation if the chains have dipoles parallel along their contour. However, the motion is differently reflected in the viscoelastic and dielectric quantities: The former reflects orientational anisotropy of stress-generating units in the chains (hereafter referred to as subchains) *at respective times*, while the latter reflects orientational correlation of the subchains *at two separate times*. Comparison of those two quantities enables us to specify details in the chain motion. In particular, for two extreme cases of incoherent and coherent subchain motion in each chain at short time scales, viscoelastic moduli G^* are explicitly calculated from relaxation times τ_p and eigenfunctions f_p for a local correlation function that represents the orientational correlation of the subchains. G_{incoh}^* and G_{coh}^* calculated for respective cases are quite different, and comparison with the G^* data specifies the coherence of the subchain motion. On the basis of these backgrounds, G^* were measured for solutions of a monodisperse *cis*-polyisoprene (PI-49; $M = 48.8$k) in oligobutadiene (OB-0.7, $M = 0.7$k) and compared with G_{incoh}^* and G_{coh}^*. (Dielectrically determined τ_p and f_p were available for the PI−49 solutions.) G_{incoh}' agreed with the G' data when the PI concentration c was less than the entanglement concentration c_e, but for $c > c_e$ significant deviation was observed. These results mean that the subchain motion is incoherent for nonentangled chains but some degree of coherence emerges for entangled chains. However, some incoherence still survived for the entangled chains even in a well-entangled state ($M/M_e \cong 10$), as evidenced from differences between the G' data and G_{coh}'. These findings were utilized to discuss the observed changes of the G^* data with c and further to re-examine conventional interpretation for those changes in terms of the Zimm/Rouse/reptation dynamics.

I. Introduction

For linear, flexible polymer chains in solutions, it has been well-known that their viscoelastic behavior changes with concentration c:[1,2] For dilute chains, the relaxation behavior is well described by Zimm/Tschoegl-type bead-spring models. This behavior changes to the Rouse-like behavior as c is increased above the overlapping concentration c^*. If the chains are sufficiently long, entanglement effects emerge and the chains further change their behavior at $c > c_e$ (entanglement concentration). Similar changes are observed also for oscillatory flow birefringence.[3−5]

The first change taking place at around c^* has been attributed to screening of the hydrodynamic and excluded volume interactions with increasing c,[1,2] and the second change at around c_e is often related to an onset of reptative motion. However, there remain some questions for these explanations, for example, a question asking whether the overlapping and interacting chains (at $c_e > c > c^*$) really obey the single-chain Rouse dynamics. To answer these questions, we need to experimentally specify details of the chain motion.

For investigation of those details, it is very important to compare several dynamic quantities that *differently* reflect the chain motion. From this point of view, dielectric quantities of so-called type-A chains having dipoles parallel along their contour are important quantities to be compared with the viscoelastic quantities. As pioneered by Stockmayer and co-workers[6,7] and later studied extensively by several groups,[8−20] global motion of type-A chains induces prominent dielectric relaxation. Fundamental features of this relaxation are determined by a local correlation function that represents orientational correlation of two portions (subchains) in a chain *at two separate times*.[14,15,18−20] This function is different in nature from a function determining the viscoelastic features, an orientation function that represents the orientational anisotropy of each subchain *at respective time*.[14,15,18,19] Because of this difference, dielectric and viscoelastic quantities reflect the same global motion in different ways and no general relationship exists between these quantities.[19] This fact in turn means that a particular relationship observed for those quantities of a system can specify details of the chain motion in that system.

Dielectric behavior has been studied for solutions of a series of *cis*-polyisoprene (PI) chains having almost identical molecular weights but differently *inverted* dipoles.[20] The behavior was analyzed to determine the eigenfunctions f_p and relaxation times τ_p for eigenmodes of the local correlation function. The dielectric mode distribution of the PI chains was broadened with increasing c ($>c^*$), and this change was essentially due to changes in the eigenfunctions.[20] These dielectric changes, if compared with viscoelastic changes, are useful for characterizing the chain motion. Specifically, the comparison enables us to examine coherence of subchain motion in each chain.[19]

On the basis of these backgrounds, we have carried out viscoelastic measurements for the PI solutions that were studied dielectrically in our previous work.[20] The measured viscoelastic moduli were compared with moduli calculated from the dielectrically determined f_p and τ_p. The results are presented in this paper. First, section II briefly explains a theoretical background for the relationships between the viscoelastic and dielectric quantities for extreme cases. Then, section IV compares

* To whom correspondence should be addressed.
† Kyoto University.
‡ Rheometric Scientific F.E. Ltd.
⊗ Abstract published in *Advance ACS Abstracts,* November 15, 1995.

0024-9297/96/2229-0097$12.00/0

the viscoelastic and dielectric data and discusses changes in the chain motion with increasing c. Finally, section V summarizes the findings of this study.

II. Theoretical Background

II.1. Microscopic Expressions for Dielectric and Viscoelastic Quantities.[14,15,18−21] We consider linear Gaussian chains of molecular weight M and concentration c.[22] Each chain is divided into N subunits referred to as subchains. The subchain considered here is a structural unit that entropically generates the mechanical stress due to its orientation. The subchain is taken to be sufficiently larger than the monomeric unit but much smaller than the chain as a whole. Global chain motion results from accumulation of the subchain motion, and features of the equilibrium chain motion are reflected in dielectric and linear viscoelastic quantities, as explained below.

For type-A chains having dipoles parallel along their contour, the dielectric relaxation at long time scales is determined by time evolution of a local correlation function,[18−20]

$$C(n,t;m) = (1/a^2)\langle \mathbf{u}(n,t)\cdot\mathbf{u}(m,0)\rangle \qquad (1)$$

Here, $\mathbf{u}(n,t)$ is a bond vector (end-to-end vector) for the nth subchain at time t and $a^2 = \langle \mathbf{u}^2\rangle$. $C(n,t;m)$ satisfies the initial and boundary conditions representing the Gaussian nature of the chain and random orientation at chain ends,[18−20]

$$C(n,0;m) = \delta_{nm}, \qquad C(n,t;m) = 0 \quad \text{for} \quad n, m = 0, N \qquad (2)$$

For the type-A chains having dipole inversion at the nth subchain, the normalized dielectric relaxation function $\Phi(t;n^*)$ (=1 at $t = 0$) and complex dielectric constant $\epsilon^*(\omega; n^*)$ at an angular frequency ω are written in terms of C,[18−20]

$$\Phi(t;n^*) = \frac{1}{N}\left[\int_0^{n^*} \mathrm{d}n - \int_{n^*}^{N} \mathrm{d}n\right]\left[\int_0^{n^*} \mathrm{d}m - \int_{n^*}^{N} \mathrm{d}m\right] C(n,t;m) \qquad (3)$$

and

$$\epsilon^*(\omega;n^*) = \epsilon_\infty - \Delta\epsilon \int_0^\infty \frac{\partial \Phi(t;n^*)}{\partial t} \exp(-i\omega t)\, \mathrm{d}t \qquad (i^2 = -1) \qquad (4)$$

Here, ϵ_∞ is the unrelaxed dielectric constant, and $\Delta\epsilon$ is the dielectric relaxation intensity: $\Delta\epsilon$ is proportional to $\nu\langle R^2\rangle$, with ν and $\langle R^2\rangle$ being the number density and mean-square end-to-end distance of the chains, respectively. (The behavior of regular type-A chains without dipole inversion is described by eqs 3 and 4 as a special case of $n^* = 0$ and/or N.)

Now, we consider linear viscoelastic relaxation of the chains at long time scales. Features of the relaxation after imposition of a small shear strain γ at time $t = 0$ are determined by time evolution of an orientation function,[15,19,21]

$$S(n,t) = (1/a^2)\langle u_x(n,t)\, u_y(n,t)\rangle \qquad (5)$$

Here, $u_\alpha(n,t)$ denotes the α (=x, y) component of the bond vector for the nth subchain. (The shear and shear-gradient directions are chosen as the x and y directions.) In general, $S(n,t)$ satisfies initial and boundary conditions representing uniform deformation at $t = 0$ and random orientation at chain ends,

$$S(n,0) = S_0 \ (n\text{-independent}) \qquad S(n,t) = 0 \quad \text{for} \quad n = 0 \text{ and } N \qquad (6)$$

The relaxation modulus $G(t)$ and dynamic modulus $G^*(\omega)$ are expressed in terms of S,[15,19,21]

$$G(t) = \frac{3\nu kT}{\gamma}\int_0^N S(n,t)\, \mathrm{d}n \qquad (7)$$

and

$$G^*(\omega) = i\omega\int_0^\infty G(t)\exp(-i\omega t)\, \mathrm{d}t \qquad (8)$$

Here, kT is the thermal energy, and the product νN represents the number density of the subchains.

Changes in $C(n,t;m)$ and $S(n,t)$ with time are induced by the same equilibrium chain motion. However, an important difference exists between C and S: As noted from eqs 1 and 5, C describes the orientational correlation of two subchains in a chain at two separate times (t and 0), while S describes the orientational anisotropy of each subchain at respective time (t). This fact means that the chain motion is differently reflected in ϵ^* and G^* (eqs 4 and 8). Consequently, there is no general relationship between ϵ^* and G^*. This in turn means that a particular relationship seen for the ϵ^* and G^* data of a system can specify details of the chain motion in that system. For two extreme cases, such relationships were derived in our previous work.[19] The results are summarized below.

II.2. Relationship between Dielectric and Viscoelastic Quantities for Extreme Cases.[19] We consider a change for a subchain bond vector $\mathbf{u}$ in a short period of time between t and $t + \Delta t$. As explained previously,[19] this change is generally determined by the chain conformation at time t and described by an equation of form

$$\mathbf{u}(n,t+\Delta t) = L^*(n;\Delta t)\,\mathbf{u}(n,t) + \Delta t\frac{1}{\zeta}\frac{\partial}{\partial \mathrm{t}}\ f_{\mathrm{B}}(n,t) \qquad (9)$$

Here, $L^*(n;\Delta t)$ is an operator for $\mathbf{u}$ at time t, ζ is the subchain friction, and f_{B} represents a random thermal force. Features of the chain dynamics determine the functional form of L^*. (The operation $L^*\mathbf{u}$ in eq 9 may involve both local and nonlocal operations.[19])

Equation 9 leads to a time evolution equation for a correlation function $S_2(n,m,t) = (1/a^2)\langle u_x(n,t)\, u_y(m,t)\rangle$ (=$S(n,t)$ for $n = m$),

$$\frac{\partial}{\partial t}S_2(n,m,t) = L_S(n,m)\, S_2(n,m,t) \qquad (10)$$

Here, L_S is an operator defined by

$$L_S(n,m) = \left.\frac{\partial\langle L^*(n;\Delta t)\, L^*(m;\Delta t)\rangle}{\partial \Delta t}\right|_{\Delta t=0} \qquad (11)$$

$S_2(n,m,t)$ satisfies the initial and boundary conditions (cf. eq 6)

$$S_2(n,m,0) = S_0\delta_{nm} \qquad S_2(n,m,t) = 0 \quad \text{for} \quad n, m = 0, N \qquad (12)$$

Similarly, a time evolution equation for $C(n,t;m)$ is

derived as

$$\frac{\partial}{\partial t}C(n,t;m) = L_C(n)\, C(n,t;m) \tag{13}$$

with the operator for C being given by

$$L_C(n) = \left.\frac{\partial\langle L^*(n;\Delta t)\rangle}{\partial \Delta t}\right|_{\Delta t=0} \tag{14}$$

Under the initial and boundary conditions, eq 2, eq 13 is solved as[19]

$$C(n,t;m) = \frac{2}{N}\sum_{p=1}^{N} f_p(n)\, f_p(m)\, \exp(-t/\tau_p) \tag{15}$$

Here, f_p and τ_p are the eigenfunction (normalized according to the initial condition, eq 2) and relaxation time for the pth eigenmode of C. f_p and τ_p are determined by

$$L_C(n)\, f_p(n) = -(1/\tau_p) f_p(n) \qquad f_p(n) = 0 \text{ for } n = 0, N \tag{16}$$

We here consider an extreme case for which subchains in each chain exhibit completely *incoherent* motion in a short period of time. (For example, the Rouse motion is classified as this type of motion.) For this case, the operator in eq 11 is decoupled as $\langle L^*(n;\Delta t)\, L^*(m;\Delta t)\rangle = \langle L^*(n;\Delta t)\rangle\langle L^*(m;\Delta t)\rangle + O(\Delta t^2)$,[19] resulting in an expression for L_S in terms of L_C (cf., eqs 11 and 14),

$$L_S(n,m) = L_C(n) + L_C(m) \tag{17}$$

Then, from eqs 10, 16, and 17, $S(n,t)$ is expanded with respect to f_p and τ_p,

$$S(n,t) = S_0\frac{2}{N}\sum_{p=1}^{N}[f_p(n)]^2 \exp(-2t/\tau_p) \tag{18}$$

Equations 15 and 18 indicate that the longest relaxation time of $S(n,t)$ is half of the time for $C(n,t;m)$ when the subchain motion is incoherent.

Using an initial condition for an affine deformation (valid for unentangled chains), $S_0 = \gamma/3$, we finally obtain an expression for reduced dynamic moduli, $G_r^* = G^*M/cRT$, for the case of incoherent subchain motion,[23]

$$G_{r,incoh}^* = 2\sum_{p=1}^{N}[\int_0^1 f_p^{\,2}\, d(n/N)]\frac{i\omega\tau_p/2}{1 + i\omega\tau_p/2} \tag{19}$$

Since slow relaxation modes dominate $G_{r,incoh}^*$ at low ω, the terminal relaxation behavior described by eq 19 is insensitive to N and thus to the choice of the subchain size. (The integral involved in eq 19 is independent of N because f_p is not separately dependent on n and N but depends only on n/N.)

We now consider the other extreme case for which the subchain motion is completely *coherent* in each chain. (For example, reptation is classified as this type of motion.) For this case, we find a relationship $\langle L^*(n;\Delta t)\, L^*(m;\Delta t)\rangle S_2(n,m,t)\rangle|_{n=m} = \langle L^*(n;\Delta t)\rangle S_2(n,n,t) + O(\Delta t^2)$.[19] This relationship leads to expressions of $S(n,t)$ and G_r^* in terms of f_p and τ_p (cf. eqs 10 and 15),

$$S(n,t) = 2S_0\sum_{p=1}^{N}[\int_0^1 f_p\, d(m/N)]f_p(n)\, \exp(-t/\tau_p) \tag{20}$$

and

$$G_{r,coh}^* = \frac{6NS_0}{\gamma}\sum_{p=1}^{N}[\int_0^1 f_p\, d(n/N)]^2\frac{i\omega\tau_p}{1 + i\omega\tau_p} \tag{21}$$

The longest relaxation time is the same for $C(n,t;m)$ and $S(n,t)$ for the case of coherent subchain motion (cf. eqs 15 and 20).

As noted from eq 21, the ω dependence of $G_{r,coh}^*$ is determined only by f_p and τ_p. However, differing from $G_{r,incoh}^*$ (eq 19), the magnitude of $G_{r,coh}^*$ is explicitly dependent on N and thus on the choice of the subchain. For terminal relaxation of entangled chains, we can naturally choose the entanglement spacing M_e as the subchain size, i.e., $N = M/M_e$. Using $S_0 = 4\gamma/15$ (Doi–Edwards initial condition[21]) for this case, we can rewrite eq 21 as

$$G_{r,coh}^* = \frac{8M}{5M_e}\sum_{p=1}^{N}[\int_0^1 f_p\, d(n/N)]^2\frac{i\omega\tau_p}{1 + i\omega\tau_p} \tag{22}$$

This result is further rewritten as a simple relationship for G'' and ϵ'' that does not explicitly involve f_p and τ_p (cf. eqs 3, 4, 7, 8, 15, and 20),

$$G''(\omega)/G_0 = \epsilon''(\omega)/\Delta\epsilon \qquad G_0 = \text{plateau modulus} \tag{23}$$

Significant differences exist between the reduced moduli for the two extreme cases (eqs 19 and 21) for both relaxation times and the relaxation mode distribution. Thus, without assuming any particular molecular model, we can specify the coherence (short-time correlation) of the subchain motion in each chain from comparison of the G_r^* data with $G_{r,incoh}^*$ and $G_{r,coh}^*$. (For the PI solutions studied here, dielectrically evaluated f_p and τ_p (p = 1–3) are available for calculation of $G_{r,incoh}^*$ and $G_{r,coh}^*$.)

III. Experimental Section

Table 1 summarizes molecular characteristics of the *cis*-polyisoprene (PI) and oligobutadiene (OB) samples. They were synthesized and characterized in our previous work.[18,20] The PI-49 sample has type-A dipoles (without inversion). Dielectric relaxation behavior has been already studied for the PI-49/OB-0.7 solutions.[20] In this study, storage and loss moduli G' and G'' were measured with a rheometer (RDA-2, Rheometrics) for the same solutions and pure OB-0.7. The PI-49 concentrations were c_{PI} (g/cm^3) = 0.027, 0.045, 0.135, 0.272, and 0.92 (bulk). For these c_{PI}, the c_{PI}/c^* ratios characterizing the overlap among the PI-49 chains were 0.8, 1.3, 4.0, 8.0, and 27.1, respectively.[20] Time–temperature superposition worked well for G^* of the solutions, and the shift factors a_T agreed with the previously obtained a_T for ϵ^*.[20] The G^* data were reduced and compared with the ϵ^* data at 40 °C.

As shown later in Figure 3, both viscoelastic and dielectric relaxation times increased with increasing c_{PI}. These changes were partly due to an increase in the monomeric friction ζ.[20] For some cases, discussion of chain motion requires a correction of ζ. However, this study compares the G^* and ϵ^* data for the same PI solution at the same temperature, and the changes in ζ with c_{PI} do not affect the comparison. For this reason, no ζ correction is carried out in this study.

IV. Results and Discussion

IV.1. Viscoelastic Behavior. Figure 1 shows G' and G'' of the PI-49/OB-0.7 solutions at 40°C. The

Table 1. Characteristics of PI and OB Samples

code	$10^{-3}M$	M_w/M_n
	cis-Polyisoprene[a]	
PI-49	48.8[b]	1.05
	oligobutadiene	
OB-0.7	0.711[c]	1.08

[a] With no inversion of type-A dipoles. [b] Weight-average molecular weight. [c] Number-average molecular weight.

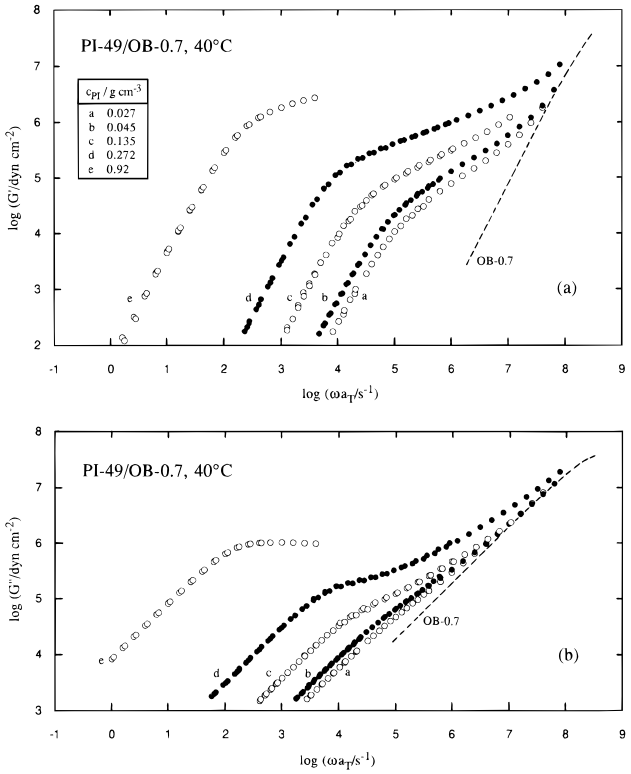

Figure 1. Master curves of G' (part a) and G'' (part b) for the PI-49/OB-0.7 solutions at 40 °C. The dashed curves indicate the behavior of pure OB-0.7.

dashed curves indicate the data obtained for the pure solvent (OB-0.7). The entanglement concentration, c_e, is 0.19 g/cm^3 for the PI-49 chains.[24]

In Figure 1, we note that PI-49 relaxes at $\omega < 10^6$ s^{-1} while OB-0.7 relaxes at much higher ω ($\geq 10^8$ s^{-1}). We also note that the viscoelastic changes with c_{PI} seen for the PI-49 solutions are quite similar to the changes for solutions in the usual low-M solvents[1,2] (like chlorinated biphenyl). Similarities were also observed for the dielectric behavior of the PI solutions in OB-0.7,[20] Isopar-G,[16] and heptane.[17]

Here, we evaluate the moduli G_{PI}* of the PI-49 chains in the solutions and quantitatively examine their changes with c_{PI}. At low $\omega < 10^6$ s^{-1} where the terminal relaxation of PI-49 is observed, OB-0.7 has a negligible contribution to G_{sol}' of the solutions (cf. Figure 1a). Thus, G_{PI}' is identical to G_{sol}'. However, for G_{sol}'' of the solutions with $c_{PI} \leq 0.135$ g/cm^3 (Figure 1b), the contribution of OB-0.7 cannot be neglected even at those low ω. We have to subtract this contribution for evaluation of G_{PI}''. As noted from the coincidence of G* for the PI-49 solutions and OB-0.7 at sufficiently high ω($>10^7$ s^{-1}), the viscoelastic stress of the solutions *additively* arises from both PI-49 and OB-0.7. This means that the OB-0.7 contribution to G_{sol}'' decreases linearly with decreasing OB-0.7 concentration c_{OB} in the solution, as is the case also for the usual homopolymer blends.[15,25] Thus, we evaluated G_{PI}'' by subtracting this

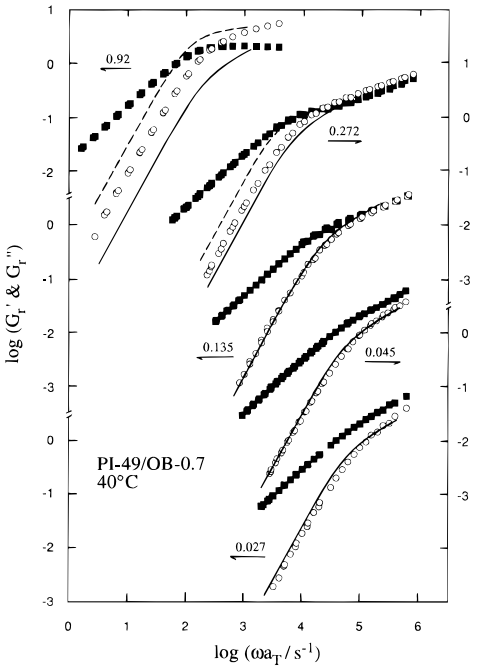

Figure 2. Comparison of the reduced moduli, $G_r^* = G_{PI}^* M_{PI}/c_{PI}RT$, for the PI-49 chains in OB-0.7: unfilled circles, G_r'; filled squares, G_r''. All data are compared at 40 °C. Solid and dashed curves indicate $G_{r,incoh}'$ (eq 19) and $G_{r,coh}'$ (eq 22) evaluated from the dielectric τ_p and f_p ($p = 1-3$) for the cases of incoherent and coherent subchain motion, respectively.

contribution as

$$G_{PI}''(\omega) = G_{sol}''(\omega) - \omega c_{OB}\eta_{OB}/\rho_{OB} \quad \text{(at low } \omega < 10^6 \text{ s}^{-1}\text{)} \quad (24)$$

Here, η_{OB} and ρ_{OB} are the viscosity and density of bulk OB-0.7. (In eq 24, we have neglected possible changes[15,25] of the OB-0.7 relaxation behavior with increasing c_{PI} (decreasing c_{OB}). However, this change becomes significant only for concentrated solutions having $G_{sol}''(\omega) \gg \omega c_{OB}\eta_{OB}/\rho_{OB}$ at low ω, and the subtraction is a very minor correction for those solutions. Thus, we can safely use eq 24 in the entire range of c_{PI}.)

Using the G_{PI}* data thus obtained, we evaluated reduced moduli of the PI-49 chains, $G_r^* = M_{PI}G_{PI}^*/c_{PI}RT$. Figure 2 shows changes in G_r* with c_{PI} (symbols). The solid and dashed curves indicate $G_{r,incoh}'$ and $G_{r,coh}'$ explained later in section IV.3.

As noted in Figure 2, the PI-49 chains with $c_{PI} = 0.027$ and 0.045 g/cm^3 ($c_{PI}/c^* = 0.8$ and 1.3) are considerably dilute and exhibit Zimm/Tschoegl-like behavior[2,21,26,27] for which G_r' (circles) and G_r'' (squares) exhibit the same power-law type ω dependence and the former is smaller than the latter at $\omega > 1/\tau_1$ (reciprocal of the longest relaxation time). For $c_{PI} = 0.135$ g/cm^3 ($c_{PI}/c^* = 4.0$), the PI-49 chains are moderately concentrated but not entangled yet. For those chains, G_r' and G_r'' still exhibit the power-law type ω dependence (weaker than the dependence seen for smaller c_{PI}) but the difference between G_r' and G_r'' vanishes at $\omega > 1/\tau_1$. This behavior is close to the Rouse behavior.[2,26,27] Finally, for $c_{PI} \geq 0.272$ g/cm^3 ($> c_e = 0.19$ g/cm^3), the PI-49 chains are entangled among themselves and the G_r' and G_r'' curves cross each other. All these changes are quite typical for solutions of flexible chains.[1,2]

IV.2. Dielectric Behavior. For the lowest three eigenmodes of $C(n,t;m)$ for the PI-49 chains dissolved in OB-0.7, we have dielectrically determined the relax-

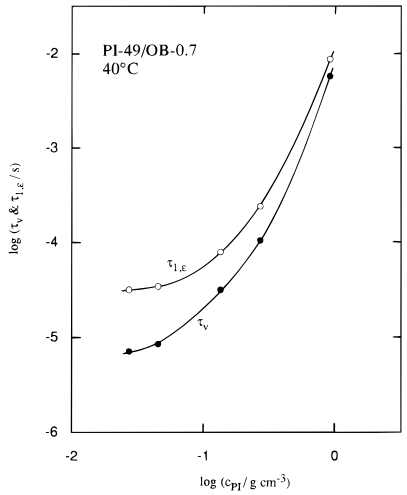

Figure 3. Concentration dependence of the dielectric and viscoelastic relaxation times, $\tau_{1,\epsilon}$ (unfilled circles) and τ_v (filled circles), for the PI-49 chains in OB-0.7 at 40 °C. $\tau_{1,\epsilon}$ is identical to the longest relaxation time for the local correlation function $C(n,t/m)$, while τ_v is 1.5−2 times shorter than the longest relaxation time $\tau_{1,G}$ for the orientation function $S(n,t)$.

ation times τ_p and integrated eigenfunctions, $F_p(n) = (\sqrt{2/N})\int_0^n f_p(m)\,dm$.[20] As done previously,[19] we numerically differentiated the F_p data to evaluate f_p.

Figure 3 demonstrates the c_{PI} dependence of $\tau_{1,\epsilon}$ at 40 °C (unfilled circles).[20] The second subscript, ϵ, explicitly indicates that $\tau_{1,\epsilon}$ is the dielectrically determined, longest relaxation time of $C(n,t;m)$. The filled circles indicate the viscoelastic relaxation time τ_v explained in the next section. We note that $\tau_{1,\epsilon}$ hardly depends on c_{PI} for $c_{PI} \le c^*$ but strongly increases for $c_{PI} > c^*$. Although not shown here, the c_{PI} dependence of $\tau_{2,\epsilon}$ and $\tau_{3,\epsilon}$ (for the second and third eigenmodes of C) was similar to that of $\tau_{1,\epsilon}$.[20] Consequently, the $\tau_{1,\epsilon}$:$\tau_{2,\epsilon}$:$\tau_{3,\epsilon}$ ratio exhibited only modest changes with c_{PI}: The ratio was 1:0.299:0.148 for the lowest $c_{PI} = 0.027$ g/cm^3 (=0.8c^*) and 1:0.257:0.135 for the highest $c_{PI} = 0.92$ g/cm^3 (=27.1c^*).[20] The ratio for the lowest c_{PI} was close to the ratio deduced from the Zimm/Tschoegl model (with the Tschoegl parameter $\epsilon_T = 0.2$), 1:0.302:0.154, and the ratio for the highest c_{PI} was in close agreement with the ratio deduced from the Rouse/reptation model, 1:0.250 (2^{-2}):0.111 (3^{-2}). A strong increase in the τ_p span with c deduced from the Muthukumar theory[28] was not observed for the dielectric data.

Figure 4 compares $f_p(n)$ for various c_{PI} (symbols). The solid curves represent sinusoidal eigenfunctions, $f_p^o = \sin(p\pi n/N)$, that are commonly deduced from the Zimm, Tschoegl, Rouse, and reptation models. For $c_{PI} = 0.027$ and 0.045 g/cm^3 ($c_{PI}/c^* = 0.8$ and 1.3) the experimental f_p values are close to the sinusoidal f_p^o, in particular for $p = 1$. However, f_p systematically deviates from f_p^o with an increase in c_{PI}, and the differences between f_p and f_p^o seen for the concentrated PI chains ($c_{PI} \ge 0.135$ g/cm^3) are far beyond uncertainties in the evaluation of f_p. Thus, as concluded in our previous paper,[20] details of the dielectric behavior of the concentrated PI-49 chains is not described by the Rouse and/or reptation models, despite the above agreement of the experimental and model τ_p span. In other words, the dielectric changes observed for the PI-49 chains are not a simple change from the Zimm/Tschoegl behavior to the Rouse/reptation behavior. Details of those dielectric changes have been discussed elsewhere.[20]

IV.3. Comparison of Dielectric and Viscoelastic Data: From the G_r^* data shown in Figure 2, an average

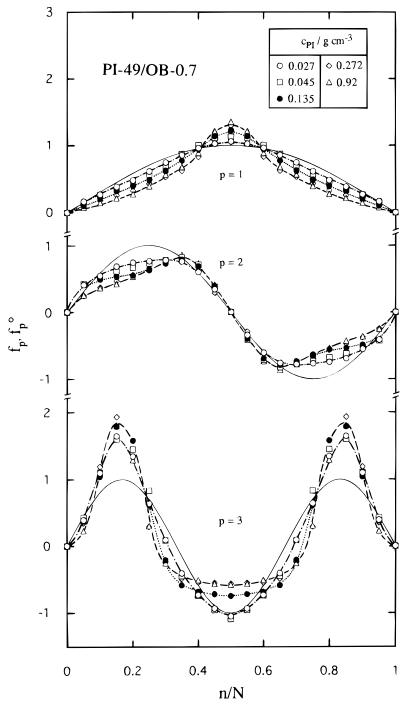

Figure 4. Comparison of the eigenfunctions f_p ($p = 1-3$) for the local correlation function of the PI-49 chains in OB-0.7. The thin, solid curves indicate sinusoidal eigenfunctions, $f_p^o = \sin(p\pi n/N)$, commonly deduced from the Zimm/Tschoegl, Rouse, and reptation models.

viscoelastic relaxation time of the PI-49 chains in OB-0.7 is evaluated as

$$\tau_v = \lim_{\omega\to 0} \frac{G_r'/\omega^2}{G_r''/\omega} \tag{25}$$

This relaxation time, frequently referred to as a *weight-average* relaxation time, is a little shorter than the longest *viscoelastic* relaxation time $\tau_{1,G}$: $\tau_{1,G}/\tau_v = 1.5-2$ for typical monodisperse polymers.

In Figure 3, τ_v at 40 °C are shown with the filled circles. We note that the c_{PI} dependence of τ_v is qualitatively similar to the dependence of the dielectric $\tau_{1,\epsilon}$. Quantitatively, τ_v is ≅4 times smaller than $\tau_{1,\epsilon}$ at small c_{PI}, and the $\tau_{1,\epsilon}/\tau_G$ ratio is reduced to ≅1.6 at large c_{PI}. Considering the above difference between $\tau_{1,G}$ and τ_v, we may estimate the ratio of the two longest relaxation times to be $\tau_{1,\epsilon}/\tau_{1,G} \cong 2$ for small c_{PI} and $\tau_{1,\epsilon}/\tau_{1,G} \cong 1$ for large c_{PI}.

As noted from eq 7, $\tau_{1,G}$ is identical to the longest relaxation time for the orientation function $S(n,t)$. Thus, the above estimates for the $\tau_{1,\epsilon}/\tau_{1,G}$ ratios at small and large c_{PI} are close to the ratios deduced for the cases of the incoherent and coherent subchain motion, respectively (cf. eqs 15, 18, and 20). However, this result is not enough to specify the coherence in the subchain motion, and we need to compare $G_{r,incoh}^*$ (eq 19) and $G_{r,coh}^*$ (eq 22) with the G_r^* data (Figure 2).

Rigorous calculation of G_r^* requires f_p and τ_p for all p, while f_p and τ_p have been experimentally determined only for $p = 1-3$.[20] Thus, we first need to examine differences between the rigorous and approximate G_r^*, the latter being calculated for $p = 1-3$. For this purpose, we compared the approximate and rigorous G_r^* for the Rouse model. The results are shown in Figure 5. As shown there, the approximate G_r'' (squares) deviates from the rigorous G_r'' (solid curve) to some

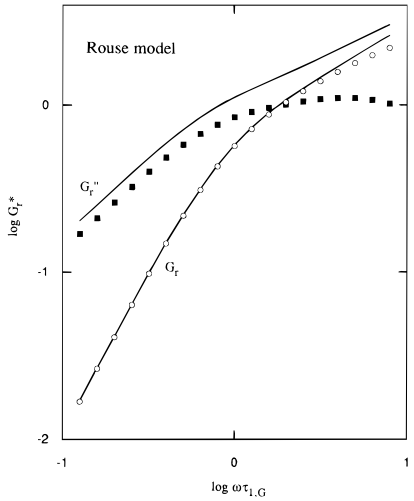

Figure 5. Comparison of the approximate reduced moduli G_r^* (symbols) evaluated for the lowest three Rouse modes with the rigorous moduli (solid curves) being contributed from all Rouse modes. Those G_r^* are plotted against a reduced frequency $\omega\tau_{1,G}$, with $\tau_{1,G}$ being the longest relaxation time for $S(n,t)$ (=longest viscoelastic relaxation time).

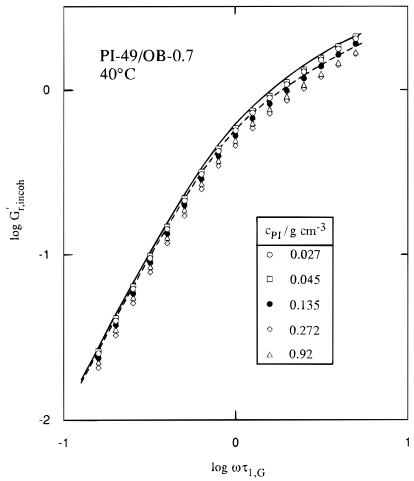

Figure 6. Comparison of the reduced storage moduli, $G_{r,incoh}'$ (symbols), evaluated from f_p and τ_p ($p = 1-3$) of the PI-49 chains for the case of incoherent subchain motion. The solid and dashed curves indicate the G_r' curves calculated for the lowest three Zimm/Tschoegl and Rouse modes, respectively. Those moduli are plotted against a reduced frequency, $\omega\tau_{1,G}$.

extent even in the flow zone at $\omega < 1/\tau_{1,G}$. However, for the approximate and rigorous G_r', satisfactory agreements are observed at $\omega \leq 6/\tau_{1,G}$. (This difference between G_r' and G_r'' reflects a fact that a contribution of fast relaxation modes is much smaller for G_r' than for G_r'' at low ω.)

The results of Figure 5 suggest that we can use the lowest three modes to satisfactorily calculate G_r' at low $\omega < 6/\tau_{1,G}$. Figure 6 compares the experimental $G_{r,incoh}'$ curves evaluated from f_p and τ_p ($p = 1-3$) for various c_{PI}. The solid and dashed curves indicate G_r' calculated for the lowest three Zimm/Tschoegl and Rouse modes. (In the ω range examined, the G_r' curves calculated for the Zimm and Tschoegl modes (with $\epsilon_T = 0.2$)[20] were almost indistinguishable.)

As seen in Figure 6, the experimental $G_{r,incoh}'$ curve is close to the Zimm/Tschoegl curve for $c_{PI} = 0.027$ and 0.045 g/cm^3 ($c_{PI}/c^* = 0.8$ and 1.3; unfilled circles and squares). However, it becomes close to the Rouse curve as c_{PI} is increased to 0.135 g/cm^3 ($c_{PI}/c^* = 4.0$; filled circles), and further changes take place at larger $c_{PI} \geq$ 0.272 g/cm^3. From these results, one may tend to attribute the change in the $G_{r,incoh}'$ curve at $c_{PI} = 0.045-0.135$ g/cm^3 to a change in the dynamic behavior of the chain from the Zimm/Tschoegl behavior to the Rouse behavior. However, f_p values at $c_{PI} = 0.135$ g/cm^3 are considerably different from the sinusoidal f_p^o for the Rouse modes (cf. Figure 4), and the observed change in $G_{r,incoh}'$ cannot be the simple Zimm/Tschoegl-to-Rouse change.

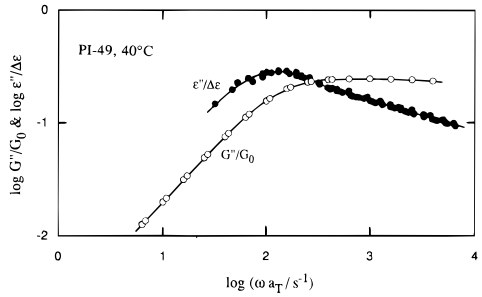

Figure 7. Comparison of $G''(\omega)/G_0$ (unfilled circles) an $\epsilon''(\omega)/\Delta\epsilon$ (filled circles) at 40 °C for bulk PI-49 ($M/M_e \cong 10$). The plateau modulus value used for reducing the G'' data was $G_0 = 4.1 \times 10^6$ dyn cm^{-2}.[29]

As done for $G_{r,incoh}'$, we evaluated $G_{r,coh}'$ (eq 22) from f_p and τ_p ($p = 1-3$). The $G_{r,incoh}'$ and $G_{r,coh}'$ curves are shown in Figure 2 with the solid and dashed curves, respectively. As noted from eqs 21 and 22, the ω dependence of $G_{r,coh}'$ is determined only by f_p and τ_p but its magnitude is dependent on the choice of the subchain size. This choice is rather arbitrary for unentangled chains. Thus, $G_{r,coh}'$ is shown only for entangled chains for which the entanglement spacing is naturally chosen as the subchain size.

In Figure 2, we first note that the G_r' data (circles) are very close to $G_{r,incoh}'$ for $c_{PI} \leq 0.135$ g/cm^3. (Although not shown here, the ω dependence was significantly different for those data and $G_{r,coh}'$). We also note that the G_r' data begin to deviate from $G_{r,incoh}'$ with an increase in c_{PI} up to 0.272 g/cm^3 and significant deviation emerges at $c_{PI} = 0.92$ g cm/^{3}. Even at this highest c_{PI}, the data do not agree with $G_{r,coh}'$.

As explained earlier, the entanglement concentration for the PI-49 chains is $c_e = 0.19$ g/cm^3. Thus, the agreement of the G_r' data with $G_{r,incoh}'$ for $c_{PI} \leq 0.135$ g/cm^3 ($<c_e$) indicates that in the nonentangled systems the subchain motion in each chain is incoherent at short time scales. On the other hand, the deviation seen for $c_{PI} \geq 0.272$ g/cm^3 ($>c_e$) means that the entanglement provides some degree of coherence to the subchain motion. However, as noted from the differences between the G_r' data and $G_{r,coh}'$ at $c_{PI} > c_e$, the incoherence still survives to some extent in the subchain motion for entangled chains. This fact is most clearly demonstrated in Figure 7 where validity of eq 23 is examined for bulk PI-49 (with $M/M_e \cong 10$). Clearly, the G''/G_0 curve is broader than the $\epsilon''/\Delta\epsilon$ curve and eq 23 does not hold. Similar differences were observed for G'' and ϵ'' of a bulk PI system with larger M(=140k; $M/M_e \cong 28$).[10] Thus, the subchain motion is not perfectly coherent even for well-entangled chains.

IV.4. Changes in the Chain Motion with *c*. In general, viscoelastic changes seen at around c^* have been explained as the Zimm/Tschoegl-to-Rouse change due to screening of the hydrodynamic and excluded volume interactions.[2] In fact, the G_r' data for the unentangled PI-49 chains agree with the calculated $G_{r,incoh}'$ curves (Figure 2), and the $G_{r,incoh}'$ curves are in

turn close to the Zimm/Tschoegl and Rouse curves at $c_{PI} \leq 1.3c^*$ and $c_{PI} = 4.0c^*$, respectively (Figure 6). However, as seen in Figure 4, the experimental eigenfunctions for $c_{PI} = 4.0c^*$ (=0.135 g/cm^3) are considerably different from the Rouse eigenfunctions. Thus, the viscoelastic changes seen at around c^* are not the simple (and conventionally considered) Zimm/Tschoegl-to-Rouse change.

The agreement between the G_r' data and $G_{r,incoh}'$ curves indicates the validity of eq 18 for $c_{PI} \leq 4c^*$. Thus, the relaxation times $\tau_p^{(S)}$ and eigenfunctions $f_p^{(S)}$ for $S(n,t)$ are given by $\tau_p/2$ and f_p^2, the latter exhibiting considerable changes as c_{PI} is increased up to $4c^*$ (cf. Figure 4). This means that the viscoelastic changes at around c^* are associated not only with the modest changes in the $\tau_p^{(S)}$ span but also with changes in $f_p^{(S)}$. It seems quite reasonable that the hydrodynamic and excluded volume interactions change with increasing c above c^*. However, the changes in these interactions do not seem to be the main cause for the observed changes in the $\tau_p^{(S)}$ span and $f_p^{(S)}$.[30] This problem deserves further attention.

The situation for the entangled chains is even more complicated. Neither $G_{r,incoh}'$ nor $G_{r,coh}'$ agrees with the G_r' data for the rather well entangled bulk PI-49 chains having $M/M_e \cong 10$ (cf. Figure 2). This result indicates that some degree of incoherence still survives in the subchain motion of bulk PI-49 chains and that the pure reptation mechanism (leading to a perfectly coherent motion) fails to explain the behavior of these chains. However, as noted from the difference between the G_r' data and $G_{r,coh}'$, eq 20 does not hold for those chains and, at this moment, $\tau_p^{(S)}$ and $f_p^{(S)}$ (for $S(n,t)$) cannot be explicitly related to τ_p and f_p (for $C(n,t;m)$). In other words, changes of $\tau_p^{(S)}$ and $f_p^{(S)}$ due to entanglements have not been specified yet. Further study is necessary for this problem.

V. Concluding Remarks

Motion of polymer chains is differently reflected in their viscoelastic and dielectric quantities. Utilizing this difference and comparing these quantities, we have specified some detailed character of the chain dynamics, coherence (or correlation) of motion of the subchains in each chain at short time scales.

For unentangled chains, the subchain motion was found to be incoherent. Those chains exhibit viscoelastic as well as dielectric changes at $c \cong c^*$ (in the nonentangled regime), but the incoherence is preserved at those changes. Those changes are essentially due to changes in the eigenfunctions $f_p^{(S)}$ and f_p for $S(n,t)$ and $C(n,t;m)$, and $f_p^{(S)}$ and f_p at $c^* < c < c_e$ are considerably different from the Rouse functions. This result means that the viscoelastic and dielectric changes seen at around c^* are not the simple Zimm/Tschoegl-to-Rouse changes. Further study is necessary for the mechanism(s) for the changes in the chain dynamics at $c \cong c^*$.

We have also found that the subchain motion becomes coherent *to some extent* as c is increased above c_e. This modest coherence (short-time correlation) of the subchain motion in each chain characterizes the entanglement dynamics. However, it should be also emphasized that some incoherence still survives even for well-entangled chains (of $M/M_e \cong 10$ or more). Those chains do not obey the reptation dynamics that leads to perfectly coherent, collective motion of the subchains (entanglement segments) along the chain contour.

Because of some incoherence remaining in the entangled chains, $f_p^{(S)}$ and $\tau_p^{(S)}$ for $S(n,t)$ of those chains could not be related to f_p and τ_p for $C(n,t:m)$. In other words, changes in $f_p^{(S)}$ and $\tau_p^{(S)}$ due to entanglement have not been specified. For further investigation of the entanglement dynamics, it would be important to experimentally determine those changes (from dichroism experiments on partially labeled chains, for example). This is considered as interesting future work.

References and Notes

(1) Johnson, R. M.; Schrag, J. L.; Ferry, J. D. *Polym. J.* **1970**, *1*, 742.

(2) Ferry, J. D. *Viscoelastic Properties of Polymers*, 3rd ed.; Wiley: New York, 1980; Chapter 9 (also see references therein).

(3) Lodge, T. P.; Miller, J. M.; Schrag, J. L. *J. Polym. Sci., Polym. Phys. Ed.* **1982**, *20*, 1409.

(4) Lodge, T. P.; Schrag, J. L. *Macromolecules* **1982**, *15*, 1376; **1984**, *17*, 352.

(5) Martel, C. J. T.; Lodge, T. P.; Dibbs, M. G.; Stokich, T. M.; Sammler, R. L.; Carriere, C. J.; Schrag, J. L. *Faraday Symp. Chem. Soc.* **1983**, *18*, 173.

(6) Stockmayer, W. H. *Pure. Appl. Chem.* **1967**, *15*, 539.

(7) (a) Baur, M. E.; Stockmayer, W. H. *J. Chem. Phys.* **1965**, *43*, 4319. (b) Stockmayer, W. H.; Burke, J. J. *Macromolecules* **1969**, *2*, 647.

(8) Imanishi, Y.; Adachi, K.; Kotaka, T. *J. Chem. Phys.* **1988**, *89*, 7585; see the references therein for the earlier work on polydisperse PI chains.

(9) Yoshida, H.; Adachi, K.; Watanabe, H.; Kotaka, T. *Polym. J. (Japan)* **1989**, *21*, 863.

(10) Adachi, K.; Yoshida, H.; Fukui, F.; Kotaka, T. *Macromolecules* **1990**, *23*, 3138.

(11) Yoshida, H.; Watanabe, H.; Adachi, K.; Kotaka, T. *Macromolecules* **1991**, *24*, 2981.

(12) Adachi, K.; Kotaka, T. *Prog. Polym. Sci.* **1993**, *18*, 585 and references therein.

(13) Boese, D.; Kremer, F.; Fetters, L. J. *Macromolecules* **1990**, *23*, 829, 1826.

(14) (a) Watanabe, H.; Yamazaki, M.; Yoshida, H.; Adachi, K.; Kotaka T. *Macromolecules* **1991**, *24*, 5365. (b) Watanabe, H.; Yamazaki, M.; Yoshida, H.; Kotaka, T. *Ibid.* **1991**, *24*, 5372.

(15) Watanabe, H.; Kotaka T. *Chemtracts: Macromol. Chem.* **1991**, *2*, 139 and refereinces therein.

(16) Patel, S. S.; Takahashi, K. M. *Macromolecules* **1992**, *25*, 4382.

(17) Urakawa, O.; Adachi, K.; Kotaka T. *Macromolecules* **1993**, *26*, 2036, 2042.

(18) Watanabe, H.; Urakawa, O.; Kotaka T. *Macromolecules* **1993**, *26*, 5073.

(19) Watanabe, H.; Urakawa, O.; Kotaka T. *Macromolecules* **1994**, *27*, 3525.

(20) Watanabe, H.; Yamada, H.; Urakawa, O. *Macromolecules* **1995**, *28*, 6443.

(21) See, for example: Doi, M.; Edwards, S. F. *The Theory of Polymer Dynamics*; Clarendon: Oxford, U.K., **1986**; Chapters 4, 6, and 7.

(22) The PI-49 chains in OB-0.7 are expanded only weakly even at the lowest c_{PI} examined.[20] Thus, we can approximate those chains as Gaussian chains.

(23) Our previous paper[19] examined constraint release of entangled chains and used the Doi−Edwards initial condition,[21] $S_0 = 4\gamma/15$. The resulting $G_{r,incoh}$* expression differs from eq 19 by a prefactor of $^4/_5$.

(24) The c_e value, 0.19 g/cm^3, was evaluated from the density ρ_{PI} and characteristic M_c^o for entanglement (=10k) for bulk PI: $c_e = \rho_{PI} M_c^o / M_{PI}$.

(25) Watanabe, H.; Yamazaki, M.; Yoshida, H.; Kotaka T. *Macromolecules* **1991**, *24*, 5573 and references therein.

(26) Tschoegl, N. W. *J. Chem. Phys.* **1964**, *40*, 473.

(27) See, for example: Yamakawa, H. *Modern Theory of Polymer Solutions*; Harper & Row: New York, 1971; Chapter 6.

(28) Muthukumar, M. *Macromolecules* **1984**, *17*, 971.

(29) Graessley, W. W. *Adv. Polym. Sci.* **1974**, *16*, 1.

(30) Watanabe, H.; Urakawa, O.; Yamada, H.; Yao, M.-L. *Macromolecules*, in press.

MA9510348